



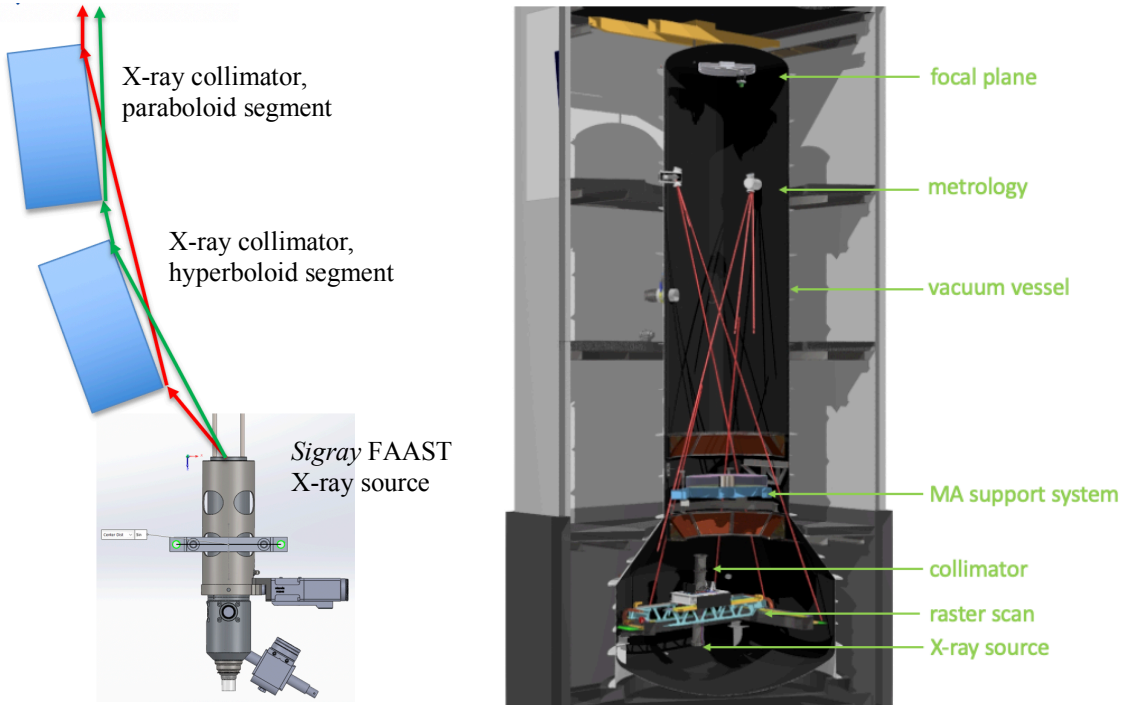
<b>Publication Year</b>	2022
<b>Acceptance in OA</b>	2023-02-01T13:25:11Z
<b>Title</b>	Global PSD tolerance for the VERT-X Wolter-I mirror
<b>Authors</b>	SPIGA, Daniele
<b>Handle</b>	<a href="http://hdl.handle.net/20.500.12386/33102">http://hdl.handle.net/20.500.12386/33102</a>
<b>Volume</b>	INAF-OAB internal report 2022/01

*INAF - Istituto Nazionale di Astrofisica  
 Osservatorio Astronomico di Brera*

## Global PSD tolerance for the VERT-X Wolter-I mirror

*Issued by D. Spiga*

*Reviewed by A. Moretti and G. Pareschi*



**Istituto Nazionale di Astrofisica (INAF)**

Via del Parco Mellini, 00100 Roma, Italy

**Osservatorio Astronomico di Brera (OAB)**

Via Brera 28, 20121 Milano, Italy

Via E. Bianchi 46, 23807 Merate, Italy

### 1. Scope of the document

In this brief note, on Medialario demand, in the context of developing the Wolter-I mirror for the VERT-X project,<sup>1</sup> we describe the global tolerances, accounting for longitudinal errors, sagittal errors and, finally, errors of the curvature radii in the longitudinal and sagittal direction.

### 2. Longitudinal and sagittal PSD

We have merged the contributions from roughness and modeled figure errors into a global tolerance PSD, aiming at a 1.2 arcsec HEW for the mirror alone, *not including parabola-hyperbola misalignments and the X-ray source extent*, as suggested by Medialario in their note of 25 June 2021. These misalignments between the two segments were already evaluated elsewhere.<sup>2</sup> The design parameters are reported in detail in the same paper, in particular the ratio of the incidence angles at the IP is set at 1.1696 value in order to abridge the length of the paraboloid. We also note that the 1.2 arcsec HEW comes from a subtraction in quadrature between the 1.3 arcsec allocated for the Wolter-I mirror itself minus 0.6 arcsec given for residual misalignments between the two mirror segments. The reference PSD we started from is represented by the final polishing status of the BEaTriX mirror, shown in Figure 1. We have assumed a similar polishing level at high frequencies but a much smoother behavior at mid-and low frequencies. This would correspond to a better figure error, as it would be measured with the MPR profilometer. This is reasonable, owing to the better quality asked of the VERT-X mirror compared to the BEaTriX mirror (a 3-fold improvement in terms of HEW). The reference PSD is displayed in Figure 1; it is made up of four connected spectral regimes in the shape of power-laws:

$$P(f) = \frac{K_n}{f^n}$$

whose parameters are listed in Table 1, and typical rms values are listed in Table 2. An “acceptable” profile, as generated from the PSDs, is shown in Figure 2.

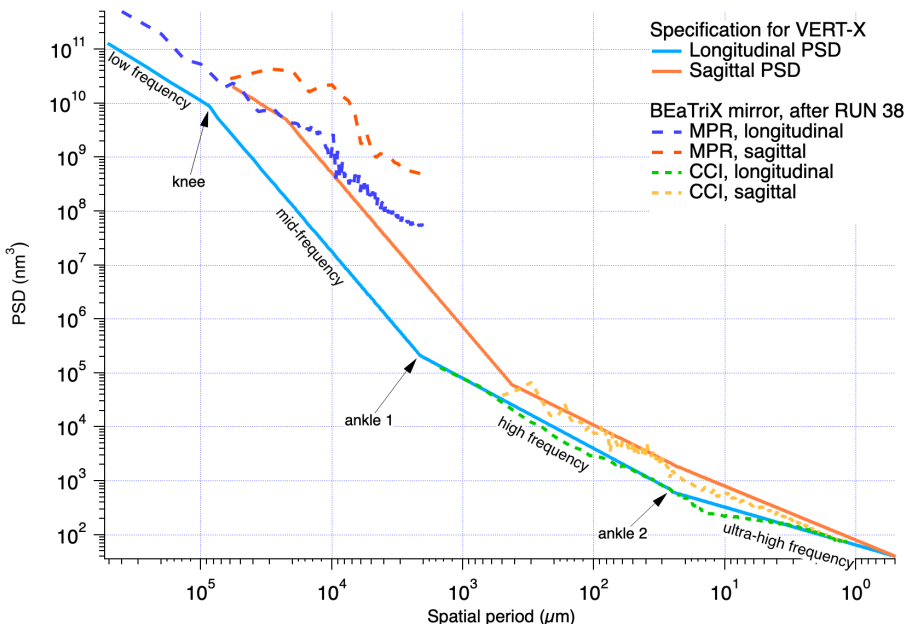


Figure 1: proposed surface roughness PSD tolerance for both segments of the VERT-X collimating mirror, for the longitudinal direction and the sagittal direction.

<sup>1</sup> A. Moretti, G. Pareschi, S. Basso, D. Spiga et al., Proc. of the SPIE, Vol. 11822, 118220K (2021)

<sup>2</sup> D. Spiga, A. Moretti, G. Pareschi et al., Proc. of the SPIE, Vol. 11822, 118220L (2021)

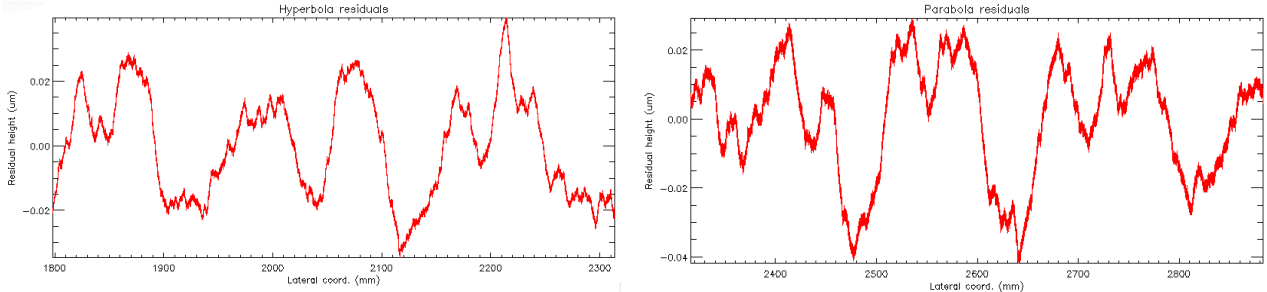


Figure 2: one of the infinitely possible profile errors in the longitudinal direction for the hyperbola (left) and the parabola (right). The profile error includes shape and roughness.

Table 1: characteristic power-law parameters of the PSD specifications, in different frequency regimes for the longitudinal and the sagittal PSDs.

PSD spec.	Longitudinal	Sagittal
Low frequency	$K_n = 350 \text{ nm}^3 \mu\text{m}^{-1.5}$ , $n = 1.5$	$K_n = 1500 \text{ nm}^3 \mu\text{m}^{-1.5}$ , $n = 1.5$
Knee wavelength	85 mm	22.5 mm
Mid-frequency	$K_n = 7 \times 10^{-5} \text{ nm}^3 \mu\text{m}^{-2.85}$ , $n = 2.85$	$K_n = 2 \times 10^{-3} \text{ nm}^3 \mu\text{m}^{-2.85}$ , $n = 2.85$
Ankle wavelength 1	1.53 mm	0.43 mm
High frequency	$K_n = 10 \text{ nm}^3 \mu\text{m}^{-1.3}$ , $n = 1.3$	$K_n = 43 \text{ nm}^3 \mu\text{m}^{-1.2}$ , $n = 1.2$
Ankle wavelength 2	25 $\mu\text{m}$	25 $\mu\text{m}$
Ultra-high frequency	$K_n = 65 \text{ nm}^3 \mu\text{m}^{-0.7}$ , $n = 0.7$	$K_n = 0.8 \text{ nm}^3 \mu\text{m}^{-1.0}$ , $n = 1.0$

Table 2: characteristic rms measured values in different bands of spatial wavelengths.

PSD spec.	MPR (500 mm - 2 mm)	Waviness (5 mm - 1 mm)	CCI 10x (1.5 mm - 2.94 $\mu\text{m}$ )	CCI 50x (300 $\mu\text{m}$ - 0.59 $\mu\text{m}$ )
Longitudinal	14.4 nm	0.52 nm	0.53 nm	0.52 nm
Sagittal	19.7 nm	2.65 nm	1.1 nm	0.75 nm

We have so generated a variable number of random profiles compatible with the PSD in Figure 1 and constructed the collimated wavefront, including the effect of profile defects at all the spatial scales.<sup>3</sup> The expected PSF is derived from the squared module of Fourier transform of the collimated wavefront. The computed HEW values are reported in Figure 3 for increasing X-ray energy up to 8 keV. The longitudinal term is clearly dominating over the sagittal one, as expected from the grazing incidence at approx. 0.4 deg. The overall HEW can be obtained combining the two contributions in quadrature (Table 3).

<sup>3</sup> L. Raimondi and D. Spiga, Astronomy and Astrophysics, Vol. 573, A22 (2015)

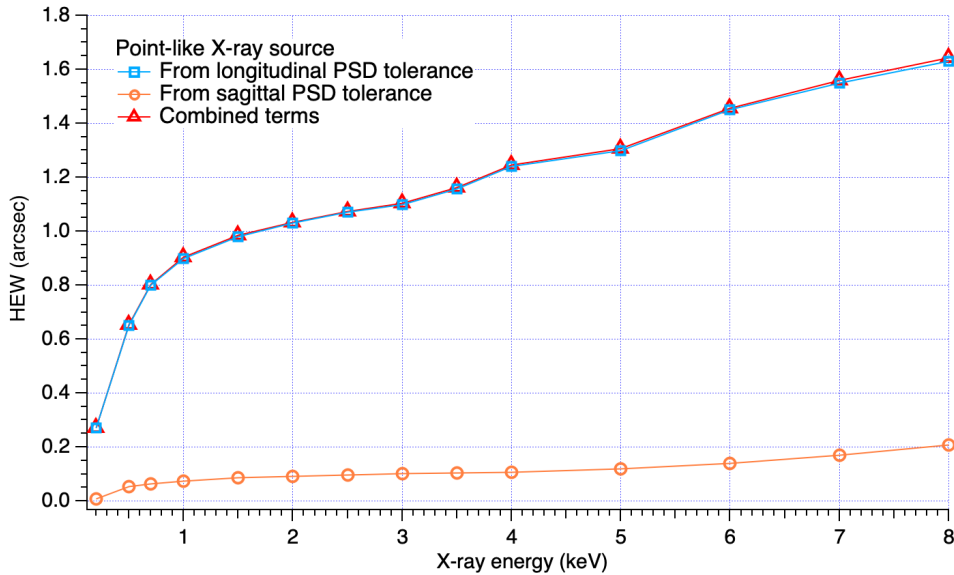


Figure 3: the expected HEW trend of the collimated wavefront as a function of the X-ray energy, as out of the VERT-X Wolter-I mirror. The longitudinal and the sagittal terms are displayed separately. The source size and parabola-hyperbola misalignments are **not** included.

Table 3: tabulated contributions to the total HEW, longitudinal and sagittal.

Energy	Longitudinal	Sagittal	Total
<b>0.2 keV</b>	0.27 arcsec	0.006 arcsec	0.270 arcsec
<b>0.5 keV</b>	0.65 arcsec	0.052 arcsec	0.652 arcsec
<b>0.7 keV</b>	0.80 arcsec	0.064 arcsec	0.802 arcsec
<b>1.0 keV</b>	0.90 arcsec	0.072 arcsec	0.903 arcsec
<b>1.5 keV</b>	0.98 arcsec	0.086 arcsec	0.984 arcsec
<b>2 keV</b>	1.03 arcsec	0.092 arcsec	1.034 arcsec
<b>2.5 keV</b>	1.07 arcsec	0.096 arcsec	1.074 arcsec
<b>3.0 keV</b>	1.10 arcsec	0.101 arcsec	1.105 arcsec
<b>3.5 keV</b>	1.16 arcsec	0.103 arcsec	1.162 arcsec
<b>4.0 keV</b>	1.24 arcsec	0.108 arcsec	1.244 arcsec
<b>5.0 keV</b>	1.30 arcsec	0.118 arcsec	1.305 arcsec
<b>6.0 keV</b>	1.45 arcsec	0.140 arcsec	1.456 arcsec
<b>7.0 keV</b>	1.55 arcsec	0.170 arcsec	1.559 arcsec
<b>8.0 keV</b>	1.63 arcsec	0.210 arcsec	1.643 arcsec

### 3. Sagittal curvature errors

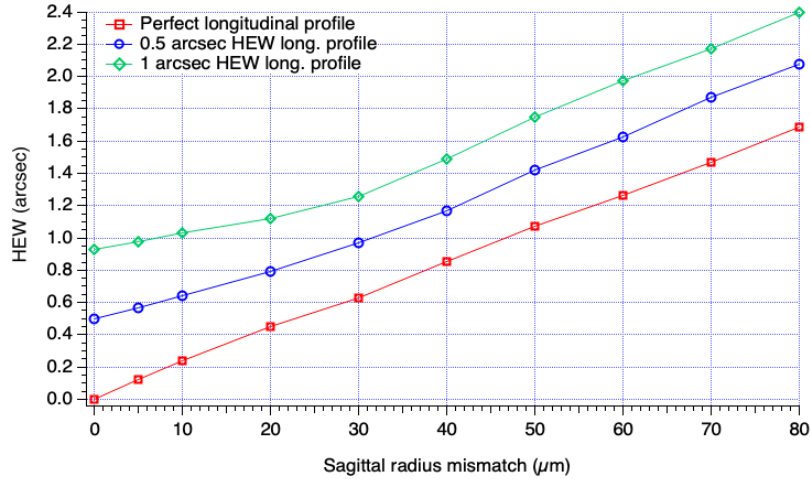


Figure 4: degradation of the HEW due to radius error in the sagittal (azimuthal) plane, for different values of the longitudinal error HEW. Only the parabolic segment error was simulated, while the hyperbola is assumed as perfect. The behavior of an error in the sole hyperbolic segment would be totally analogous.

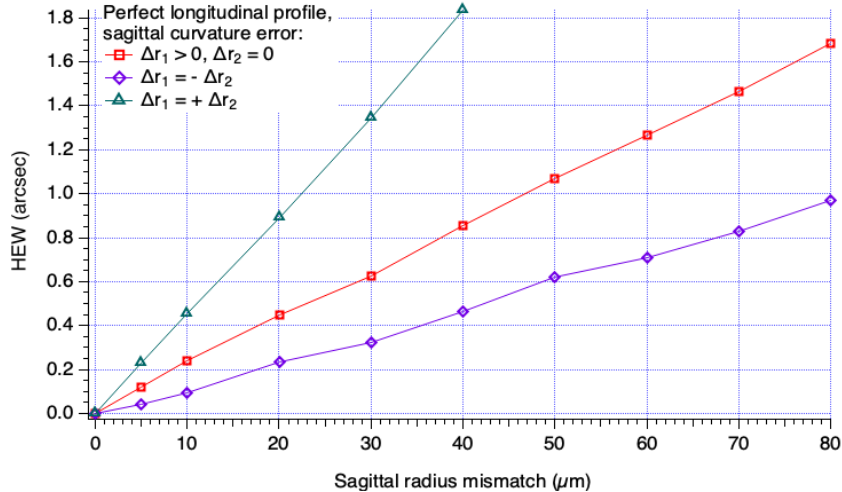


Figure 5: degradation of the HEW due to radius error in the sagittal (azimuthal) plane, for a perfect longitudinal profile. Besides the sole parabola error effect (red line, as in Figure 4), opposite errors in the parabola and the hyperbola (purple) compensate the aberration, while curvature errors with the same sign make it approx. double.

In Figure 4, we show the simulation of the expected aberrations from an error in the sagittal radius, i.e. in the azimuthal curvature radius of a single segment, either parabolic or hyperbolic. The simulation was performed in 2D,<sup>4</sup> also accounting for different possible errors in the mirror shape (as analysed in Sect. 2). Besides the expected linear increase for a perfect mirror (red line), there is also a contribution from the figure error, which brings the HEW value to higher values. The increase is roughly linear also (i.e., the total HEW is the linear sum of the figure error and of the sagittal radius error) *but for small radial errors (< 30 μm)* the combination between the two terms exhibits a slightly flatter trend.

<sup>4</sup> D. Spiga, A. Moretti, G. Pareschi, et al., Proc. of SPIE, Vol. 11822, 118220L (2021)

As a first glance, the tolerance in the sagittal radius **would be very strict** ( $10 \mu\text{m}$  to avoid a degradation of the HEW larger than  $0.1 \text{ arcsec}$  if we stick to the green line). Nevertheless, we have two chances to can relax this prescription:

- an error in the sagittal curvature of the parabola can be *somewhat* corrected by an opposite radius error of the hyperbola, although **not very effectively** (Figure 5);
- as the effect of curvature radius errors results in a change of focal length, the detector can be re-focused to correct the focus and so retrieve the expected HEW, excepting a remaining astigmatism term. The re-focusing is *mostly effective at minimizing the residual astigmatism when the errors in the sagittal radius are the same* for the parabolic and the hyperbolic segment (Figure 6). This is true also in the presence of non-ideal longitudinal profiles (Figure 7, assuming a  $1 \text{ arcsec}$  HEW for longitudinal profiles). We can also see that, for such an optic, the degradation of the HEW is negligible – upon refocusing – up to radius errors of  **$50 \mu\text{m}$** , provided that the two radii of curvature coincide within  **$20 \mu\text{m}$**  (Figure 8).

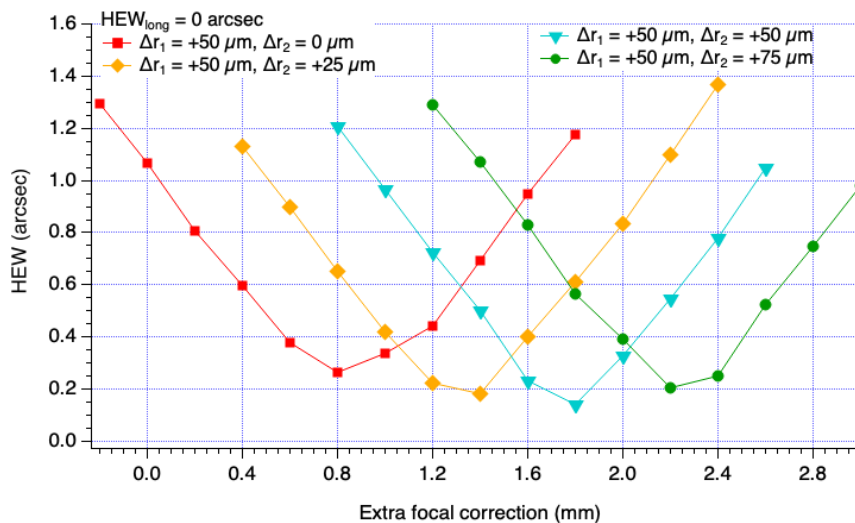


Figure 6: best focus search for different errors in the sagittal curvature of the hyperbolic segment. The error in the sagittal curvature for the parabolic mirror is always  $50 \mu\text{m}$ . The longitudinal profiles are assumed as perfect. The best option for refocusing is when the curvature radii are the same.

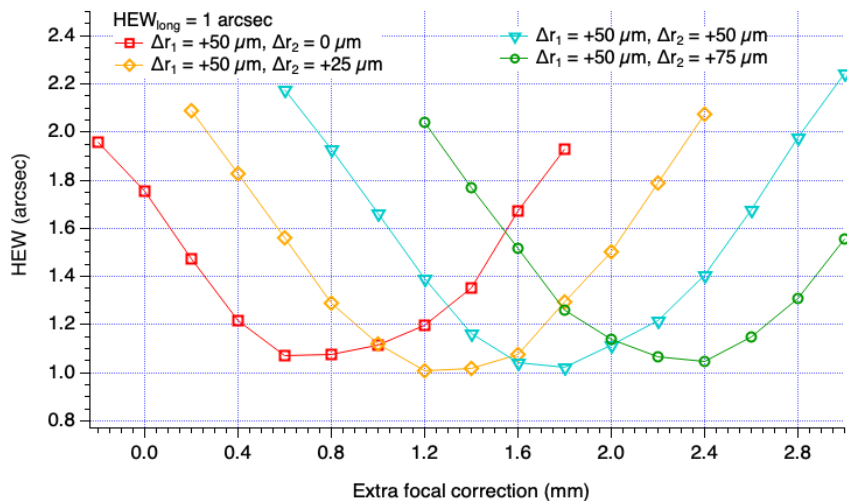


Figure 7: best focus search for different errors in the sagittal curvature of the hyperbolic segment. The error in the sagittal curvature for the parabolic mirror is always  $50 \mu\text{m}$ . The longitudinal profile errors are assumed to return a  $1 \text{ arcsec}$  HEW term.

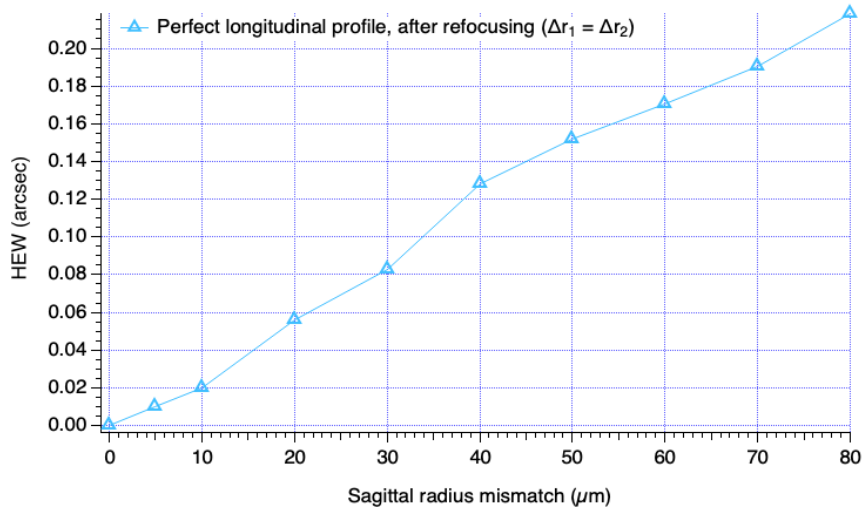


Figure 8: refocused HEW as a function of the sagittal error radius error, in the assumption that it takes on the same value for the parabola and the hyperbola.

#### 4. Longitudinal curvature errors

Even if an analysis of the longitudinal curvature error is already included in the tolerances discussed in Sect. 2 (i.e., computing the PSD of the profile error also includes the curvature error), errors in the longitudinal and sagittal curvature radii can be correlated to return astigmatism-free optics via re-focusing. To that end, the longitudinal radius and the sagittal radius have to fulfil the *pseudo-Rowland* condition:

$$R_{lon} = \frac{R_{sag}}{\sin^2 \alpha_{inc}}$$

meaning that the longitudinal radius has to be determined to the same percent of accuracy as the sagittal radius (always assumed to be the same for the parabolic and the hyperbolic segment). In particular, an error in  $R_{sag}$  can be exactly corrected changing  $R_{lon}$ , paying the price of a *slightly* different focal length  $f = R_{sag}/\tan(4\alpha_{inc})$ .

#### 5. Conclusions

This document summarized some preliminary formulation for the fabrication tolerances for the VERT-X Wolter-I collimator. PSDs for the longitudinal and sagittal polishing and figuring have been provided in order to keep the HEW < 1.2 arcsec below 3.5 keV (not including the X-ray source size, that is assumed to be well characterized and removable by deconvolution). Fabrication tolerances for the sagittal radii (< 50 μm and coincident within 20 μm) have been designed in order to make their effect negligible provided that the focal length can be corrected. The error in the sagittal radii can even vanish, if the longitudinal curvature error can be corrected to match the actual value of the sagittal radius according the pseudo-Rowland condition and correcting the focal length by the requested amount.